

See discussions, stats, and author profiles for this publication at: <https://www.researchgate.net/publication/307593680>

# Influence of Lipid Core Material on Physicochemical Characteristics of Ursolic Acid Loaded Nanostructured Lipid Carrier: An Attempt to Enhance Anticancer Activity

Article in Langmuir · September 2016

DOI: 10.1021/acs.langmuir.6b02402

---

CITATIONS

46

11 authors, including:



Gourab Karmakar

University of North Bengal

15 PUBLICATIONS 248 CITATIONS

[SEE PROFILE](#)

---

READS

280



Biplab Roy

Luleå University of Technology

19 PUBLICATIONS 290 CITATIONS

[SEE PROFILE](#)



Pritam Guha

Polymer Institute SAS

19 PUBLICATIONS 276 CITATIONS

[SEE PROFILE](#)



Shila Elizabeth Besra

Indian Institute of Chemical Biology

53 PUBLICATIONS 796 CITATIONS

[SEE PROFILE](#)

# Influence of Lipid Core Material on Physicochemical Characteristics of an Ursolic Acid-Loaded Nanostructured Lipid Carrier: An Attempt To Enhance Anticancer Activity

Prasant Nahak,<sup>†</sup> Gourab Karmakar,<sup>†</sup> Priyam Chettri,<sup>‡</sup> Biplab Roy,<sup>†</sup> Pritam Guha,<sup>†</sup> Shila Elizabeth Besra,<sup>§</sup> Anjana Soren,<sup>§</sup> Alexey G. Bykov,<sup>||</sup> Alexander V. Akentiev,<sup>||</sup> Boris A. Noskov,<sup>||</sup> and Amiya Kumar Panda<sup>\*†</sup>

<sup>†</sup>Department of Chemistry, University of North Bengal, Darjeeling 734 013, West Bengal, India

<sup>‡</sup>Department of Biotechnology, University of North Bengal, Darjeeling 734 013, West Bengal, India

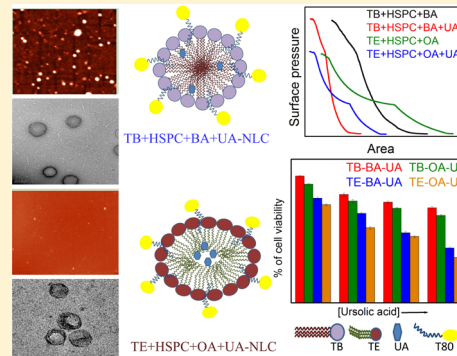
<sup>§</sup>Cancer Biology and Inflammatory Disorder Division, CSIR-Indian Institute of Chemical Biology, 4, Raja S. C. Mullick Road, Kolkata 700032, West Bengal, India

<sup>||</sup>Department of Colloid Chemistry, St. Petersburg State University, Universitetsky pr. 26, 198504 St. Petersburg, Russia

<sup>\*</sup>Department of Chemistry and Chemical Technology, Vidyasagar University, Midnapore 721 102, West Bengal, India

## S Supporting Information

**ABSTRACT:** The impact of saturation and unsaturation in the fatty acyl hydrocarbon chain on the physicochemical properties of nanostructured lipid carriers (NLCs) was investigated to develop novel delivery systems loaded with an anticancer drug, ursolic acid (UA). Aqueous NLC dispersions were prepared by a high-pressure homogenization–ultrasonication technique with Tween 80 as a stabilizer. Mutual miscibility of the components at the air–water interface was assessed by surface pressure–area measurements, where attractive interactions were recorded between the lipid mixtures and UA, irrespective of the extent of saturation or unsaturation in fatty acyl chains. NLCs were characterized by combined dynamic light scattering, transmission electron microscopy (TEM), atomic force microscopy (AFM), differential scanning calorimetry, drug encapsulation efficiency, drug payload, *in vitro* drug release, and *in vitro* cytotoxicity studies. The saturated lipid-based NLCs were larger than unsaturated lipids. TEM and AFM images revealed the spherical and smooth surface morphology of NLCs. The encapsulation efficiency and drug payload were higher for unsaturated lipid blends. *In vitro* release studies indicate that the nature of the lipid matrix affects both the rate and release pattern. All UA-loaded formulations exhibited superior anticancer activity compared to that of free UA against human leukemic cell line K562 and melanoma cell line B16.



## INTRODUCTION

Cytotoxic anticancer drugs are more reactive, more unstable, and more diverse in terms of molecular structure and physicochemical properties than other drug classes. At the same time, their poor specificity and tendency to induce drug resistance hinder the optimal performance in the case of conventional chemotherapy. Cancer cells exercise a variety of defense mechanisms at the cellular level to diminish the activities of chemotherapeutic agents to which they are exposed. These defense mechanisms are known as “cellular” drug resistance. The most notable is the multidrug resistance (MDR) phenotype, which involves active efflux of a broad range of cytotoxic drug molecules out of the cytoplasm by membrane-bound transporters.<sup>1–3</sup> In recent years, it has become more evident that the mere development of novel drugs is insufficient to guarantee progress in drug therapy.

Nanodimensional drug delivery systems possess important properties such as the increasing solubility of hydrophobic drugs and the improvement of their bioavailability.<sup>4,5</sup> Solid lipid

nanoarticles (SLNs) combine the advantages of emulsions, liposomes, and polymeric nanoparticles; other favorable qualities of SLNs include biocompatibility,<sup>6</sup> improved solubility, high bioavailability, controlled drug release,<sup>7,8</sup> targeting effect on brain,<sup>9</sup> accessibility to large scale production,<sup>10</sup> etc. It is therefore not surprising that this relatively new class of drug carriers is quickly being adopted for the delivery of various anticancer compounds as the SLNs, comprising physiological lipids, can minimize potential toxicity and enhance efficiency.<sup>11</sup> However, because of the highly crystalline nature of pure solid lipids or blends of solid lipids, drugs tend to be excluded, leading to low loading capacity and drug expulsion during storage. To overcome the limitations of SLNs, nanostructured lipid carriers (NLCs) have evolved as alternatives. NLCs are usually prepared from a mixture of spatially incompatible solid

Received: June 28, 2016

Revised: August 16, 2016

Published: September 2, 2016

and liquid lipids. Assimilation of liquid lipids increases the imperfections in the solid lipid matrix; furthermore, liquid lipids can elevate the level of drug solubilization, allowing superior accommodation for the hydrophobic drugs, which eventually enhances the drug payload and reduces the level of expulsion of the drug during storage.<sup>12–15</sup> A blend of solid and liquid lipids can form a stable NLC that remains in the solid state at body temperature; thus, the drug release profile can be easily modulated by varying the lipid matrix composition.<sup>16,17</sup> More important is the faster internalization of lipid nanoparticles into cancerous cells, leading to greater potential in cancer therapy.<sup>18–20</sup>

NLCs comprising a mixture of saturated (solid) and unsaturated (liquid) triglycerides, phospholipids, and fatty acids may be considered as an interesting alternative to conventional combinations such as fatty acid and triglyceride, as the blends are usually polycrystalline in nature and can enhance physical stability, encapsulation efficiency, release behavior, therapeutic efficiency, etc.<sup>17,19,21,22</sup> Although a number of reports about NLCs comprising saturated (solid) and unsaturated (fluid/liquid) lipids are available in the literature,<sup>12–14,23</sup> comparative studies describing the effect of unsaturated lipids and saturated lipids on the physicochemistry of NLCs are scarce. Thus, there has been ample research in the field of NLCs, with special reference to the use of different combinations of saturated and unsaturated lipids.

Ursolic acid (UA, 3 $\beta$ -hydroxy-urs-12-en-28-oic acid), a natural pentacyclic triterpenoid found in different plant species,<sup>24</sup> possesses a wide range of bioactivities, viz., antitumor, anti-inflammatory, antioxidant, antibacterial, antiviral, and hepatoprotective effects.<sup>25–29</sup> Recent studies have shown that UA has potential antitumor effects and cytotoxic activity toward various types of cancer cell lines.<sup>30–33</sup> In spite of such potential, the clinical application of UA is limited because of its poor aqueous solubility, resulting in its low bioavailability and poor *in vivo* pharmacokinetics. During the past decade, many approaches have been developed to improve the solubility of UA using polymeric nanoparticles,<sup>32–35</sup> micronization,<sup>36</sup> lipidic nanoparticles,<sup>37,38</sup> liposomes,<sup>30,39</sup> salt formation,<sup>40</sup> solid dispersions,<sup>40</sup> inclusion complexes,<sup>41,42</sup> microemulsions and nanocrystals, etc.<sup>31</sup> In spite of different attempts, it has not yet been possible to develop a single optimal delivery system. Therefore, the search for novel drug delivery systems is highly warranted to improve the solubility, payload, and oral bioavailability of UA. The aim of this study was to evaluate and compare the saturated and unsaturated lipid comprising NLCs to determine if differences in composition can alter the performance of these systems. Saturated lipid [tribehenin (TB) and 2,3-di-(docosanoyloxy)propyl docosanoate], unsaturated lipid (trierucin (TE) and 2,3-bis{[(Z)-docos-13-enoyl]oxy}propyl (Z)-docos-13-enoate], saturated fatty acid [behenic acid (BA), docosanoic acid], and unsaturated fatty acid [oleic acid (OA), (9Z)-9-octadecenoic acid] were used for these studies, keeping the molar proportion of HSPC (hydrogenated soy phosphatidylcholine) constant for all the systems. Because the major drawbacks of ursolic acid are lower drug loading and poor water solubility, another objective was the development of UA-encapsulated NLCs comprising different lipid matrices to enhance drug loading, improve solubility, and increase oral bioavailability.

Surface pressure-area isotherm studies of the pure and mixed lipids as well as with ursolic acid in different combinations were conducted to determine the nature of the

interactions between the lipids and the drug. Such studies can also predict the location of the drug molecules. If UA molecules prefer to stay at the interface of the NLCs, they would definitely alter the surface pressure-area isotherm of the lipid mixture. On the other hand, if the drug molecules prefer to stay in the core of the NLCs, they would hardly have any impact on the surface pressure-area isotherm of lipid mixtures. To address this issue, surface pressure-area isotherms of the lipid mixtures with varying amounts of UA were determined. The influence of different lipids on the size, polydispersity index, and  $\zeta$  potential of NLCs was investigated in the absence and presence of UA. Calorimetric studies of different formulations in the absence and presence of UA were conducted with the intention of determining the impact of the composition of lipids as well as UA on the thermal behavior of NLCs. To investigate the impact of saturated and unsaturated lipids on UA entrapment efficiency (EE), loading content (LC) and release kinetics of UA-loaded formulations were also assessed. Finally, anticancer activities against human leukemic cell line K562 and melanoma cell line B16 were evaluated to determine the anticancer potential of UA-loaded NLCs. It is believed that such a comprehensive study would eventually lead to the formulation of novel drug delivery systems in the treatment of cancer and to a clearer understanding of the fundamental properties of NLCs.

## MATERIALS AND METHODS

**Materials.** Ursolic acid (UA), tribehenin (TB), trierucin (TE), behenic acid (BA), and oleic acid (OA) were purchased from TCI Chemicals. Hydrogenated soy phosphatidylcholine (HSPC), a dialysis bag (12 kDa molecular weight cutoff), DMEM, and RPMI 1640 medium with L-glutamine (Gibco), fetal calf serum, sodium pyruvate, HEPES, MTT [3-(4,5-dimethylthiazol-2-yl)-2,5-diphenyltetrazolium bromide], and trypsin were obtained from Sigma-Aldrich. Tween 80 was purchased from Sisco Research Laboratory. AR grade disodium hydrogen phosphate ( $\text{Na}_2\text{HPO}_4 \cdot 2\text{H}_2\text{O}$ ), sodium dihydrogen phosphate ( $\text{NaH}_2\text{PO}_4 \cdot 2\text{H}_2\text{O}$ ), and sodium chloride (NaCl) were the products of Merck Specialties Pvt. Ltd. Penicillins/streptomycin (Biowest), gentamycin (Nicholas), dimethyl sulfoxide (DMSO), sodium bicarbonate, and other chemicals/reagents were of analytical grade and purchased from local firms. All the chemicals used were stated to be  $\geq 99\%$  pure and used as received. Doubly distilled water and high-performance liquid chromatography grade water were used throughout the study. Human leukemic cell line K562 and mouse melanoma cell line B16 were purchased from the National Facility for Animal Tissue and Cell Culture (Pune, India). The K562 cells were maintained in RPMI 1640, and B16 cells were maintained in DMEM supplemented with 10% heat-inactivated FCS, 100 units/mL penicillin, 100 mg/mL streptomycin, and 100  $\mu\text{g}/\text{mL}$  gentamycin. Both cultures were maintained at 37 °C in a humidified atmosphere containing 5% CO<sub>2</sub>. Mouse melanoma B16 cells are adherent in nature. During subculturing of the cells, this adherence can be diminished by adding a 1× trypsin solution to the cell. In all the experiments, untreated leukemic and melanoma cells were termed the control group.

**Methods.** Surface pressure ( $\pi$ )–area ( $A$ ) isotherms of pure as well as mixed monolayers (solvent spread) were obtained using a Langmuir surface balance (Micro Trough X, Kibron, Helsinki, Finland). A monolayer was generated by spreading an appropriate quantity of a lipid solution dissolved in a 3:1 (v/v) chloroform/methanol mixture at the air–water interface with a Hamilton microsyringe. The solvent was allowed to evaporate for 15 min. After the generation and equilibration of the monolayer film, the barriers were compressed at a rate of 5 mm/min.

NLCs were prepared by the hot homogenization–ultrasonication method as previously described.<sup>43</sup> Briefly, quantitative amounts of lipids (2.2:1 TB/TE:HSPC:OA/BA molar ratio) were dissolved in a 3:1 (v/v) chloroform/methanol mixture; the solvent was removed

using a rotary evaporator. The thin film thus obtained was melted at 95 °C and dispersed in the preheated aqueous surfactant (Tween 80) solution. The coarse emulsion was exposed to high-speed dispersion for 1 h; the obtained pre-emulsion was sonicated for a period of 1 h with a probe sonicator (Takashi U250, Takashi Electric) at 150 W/kHz, maintaining the same temperature to produce nanoemulsions that were allowed to cool to room temperature to produce the NLCs, which were stored at 4 °C for further study. In the case of the drug-loaded formulation, UA was premixed with the lipids while the thin film was being generated. The total lipid concentration in the dispersion was maintained at 5 mM in a 2:2:1 TB/TE:HSPC:OA/BA molar ratio, and a 10 mM aqueous nonionic (Tween 80) surfactant solution was used as a stabilizer. Different formulations, drug free or loaded, were prepared. The drug concentrations were 0.125, 0.25, and 0.5 mM for all cases.

The mean particle size, population distribution, polydispersity index, and  $\zeta$  potential of the NLCs were measured in a dynamic light scattering spectrometer using a Malvern Zetasizer Nano Series ZS90 instruments (Malvern Instruments, Malvern, U.K.) at 25 °C. The shape, morphology, and surface topology of the NLCs were investigated by transmission electron microscopy (TEM) (Hitachi, Tokyo, Japan) and tapping mode atomic force microscopy (AFM) (Nanoscope III, Bruker) studies.<sup>43</sup> Calorimetric measurements were performed using a differential scanning calorimetry (DSC) 1 STAR<sup>e</sup> system (Mettler Toledo). The DSC studies were performed in the temperature range of -30 to 100 °C with a scan rate of 2.5 °C/min. The phase transition temperature and other relevant thermal parameters were evaluated from the obtained DSC thermograms of respective samples using STAR<sup>e</sup> Software version 11.00. The entrapment efficiency (EE) and drug loading (DL) were determined by the standard methods as reported previously.<sup>44</sup> The UA content was estimated with a UV spectrophotometer, measuring the absorbance at 214 nm. The entrapment efficiency (EE) and drug loading (DL) capacity of NLCs were calculated using the following equations:

$$\text{EE\%} = \frac{W_{\text{TC}} - W_{\text{FC}}}{W_{\text{TC}}} \times 100 \quad (1)$$

$$\text{DL\%} = \frac{W_{\text{TC}} - W_{\text{FC}}}{W_{\text{TC}} - W_{\text{FC}} + W_{\text{TL}}} \times 100 \quad (2)$$

where  $W_{\text{TC}}$ ,  $W_{\text{FC}}$ , and  $W_{\text{TL}}$  represent total amounts of UA, free UA, and lipid, respectively. *In vitro* release of UA from the NLCs was assessed using the standard dialysis bag method under sink conditions over a 96 h period.

**In Vitro Cytotoxicity Study of UA-Loaded NLCs.** Log phase K562 and B16 cells ( $1 \times 10^5$  cells, 100  $\mu\text{L}$  cell suspensions) were seeded in 96-well tissue culture plates. They were treated with freshly prepared UA-loaded NLCs at different concentrations and different incubation times at 37 °C in a humidified atmosphere containing 5% CO<sub>2</sub>. Untreated cells served as the control. The cytotoxicity studies were performed using the MTT assay, and the absorbance of the colored solution was measured at a wavelength of 492 nm for K562 and at 570 nm for B16 cells by a microplate manager (reader type, model 680 XR from Bio-Rad Laboratories Inc.). IC<sub>50</sub> values were obtained at 24 and 48 h for UA-loaded NLCs.

## RESULTS AND DISCUSSION

**Interfacial Behavior of Monomolecular Films.** Surface pressure ( $\pi$ )–area (A) isotherms were constructed for pure components, mixed lipids, and mixed lipids in combination with UA. In the case of the mixed lipid and UA combinations, the lipid mixture was considered component 1 while UA was considered component 2. Lift-off areas of TB, TE, HSPC, BA, OA, and UA appeared at 75.14, 164.02, 93.61, 51.22, 78.87, and 106.17  $\text{nm}^2 \text{molecule}^{-1}$ , respectively. Representative isotherms are shown in Figure 1 and Figure S1.

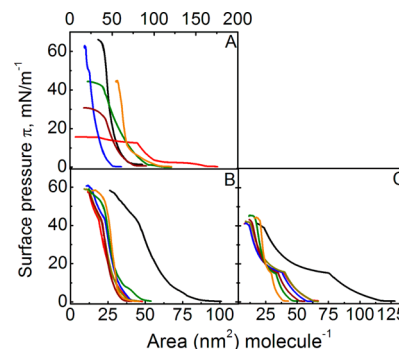


**Figure 1.** Surface pressure ( $\pi$ )–area (A) isotherms of (A) (black) tri behenin, (red) trierucin, (green) HSPC, (blue) behenic acid, (brown) oleic acid, and (orange) ursolic acid; (B) a TB/HSPC/BA mixture; and (C) a TE/HSPC/OA mixture. Panels B and C describe the  $\pi$ -A isotherm of the mixed monolayer in the absence and presence of ursolic acid using water as the subphase. The mole percents of ursolic acid with respect to the lipid mixture were (black) 0, (red) 2.5, (blue) 5, (brown) 10, (maroon) 30, (green) 50, and (orange) 70. The temperature was 25 °C.

Addition of UA resulted in a downshift in the lift-off area of the mixed monolayers; the downshift was more significant for fluid lipids (TE/HSPC/OA and TE/HSPC/BA). The condensing effect of UA, analogous to that of cholesterol,<sup>45–48</sup> was due to the strong attractive hydrophobic and/or van der Waals interactions between the lipids and UA molecules.

Monolayer mechanical properties can easily be assessed by calculating the elasticity modulus ( $C_s^{-1}$ ), which is the inverse of the film compressibility defined according to the following relation<sup>49</sup>

$$C_s^{-1} = -A \left( \frac{d\pi}{dA} \right)_T \quad (3)$$

The profiles of the elasticity modulus versus the percent of compressed area are shown in Figure 2.

For lipid mixtures in the absence of UA, maximal values were observed at 85, 79, 46, and 37  $\text{mN m}^{-1}$  for TB/HSPC/BA, TB/HSPC/OA, TE/HSPC/BA, and TE/HSPC/OA mixtures, respectively.  $C_s^{-1}$  values for UA/lipid mixed monolayers reveal a major reduction in the maximum, ranging from 120 to 67  $\text{mN m}^{-1}$ , from 95 to 65  $\text{mN m}^{-1}$ , from 75 to 30  $\text{mN m}^{-1}$ , and from

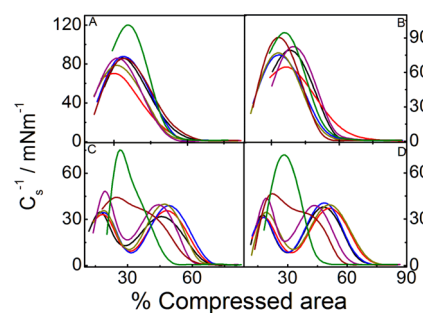


**Figure 2.** Variation of the inelasticity modulus ( $C_s^{-1}$ ) with the percent of compressed area for mixed monolayer systems: (A) TB/HSPC/BA, (B) TB/HSPC/OA, (C) TE/HSPC/BA, and (D) TE/HSPC/OA. The lipid mixture was component 1 [2:2:1 (m/m/m)], and ursolic acid was component 2. The mole percents of ursolic acid with respect to the lipid mixture were (black) 0, (red) 2.5, (blue) 5, (brown) 10, (purple) 30, (maroon) 50, and (green) 70. The temperature was 25 °C.

72 to 35 mN m<sup>-1</sup> for TB/HSPC/BA, TB/HSPC/OA, TE/HSPC/BA, and TE/HSPC/OA mixtures, respectively. Such a decrease indicates a fluidizing effect of UA or the decreased elasticity of the mixed lipid monolayer; the lower the maximal value of the elasticity modulus, the higher the fluidity of the monolayer.<sup>50</sup> An alteration of the molecular area of the UA molecule occupied in the monolayer, a change in the molecular packing effectiveness, and/or a change in the membrane fluidity may induce such modifications in the thermodynamic parameters.

To gain further information about the interactions between the lipids and UA molecules, the excess area ( $A_{\text{ex}}$ ), changes in the excess free energy of mixing ( $\Delta G_{\text{ex}}$ ), and changes in the free energy of mixing ( $\Delta G_{\text{mix}}$ ) of the lipid/UA monolayers were calculated from the  $\pi$ - $A$  isotherms at different surface pressures. The excess area determines if the mixing is ideal or nonideal. The ideal area of mixing is calculated using eq 4:<sup>50</sup>

$$A_{\text{id}} = x_1 A_1 + x_2 A_2 \quad (4)$$

where  $x_1$  and  $x_2$  are the mole fractions and  $A_1$  and  $A_2$  the areas per molecule of components 1 and 2, respectively. To estimate the deviation from the ideal behavior, the excess area ( $A_{\text{ex}}$ ) was calculated as<sup>50</sup>

$$A_{\text{ex}} = A_{12} - A_{\text{id}} \quad (5)$$

where  $A_{12}$  represents the experimentally obtained mean molecular area. The  $A_{\text{ex}}$  value of the pseudobinary monolayer was calculated at different surface pressures (from 5 to 30 mN m<sup>-1</sup> with an interval of 5 mN m<sup>-1</sup>), as shown in Figure 3.

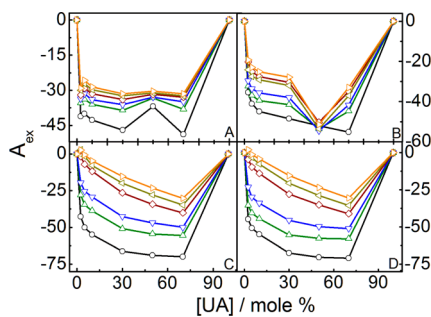


**Figure 3.** Dependence of the excess molecular area ( $A_{\text{ex}}$ ) on the relative proportion of ursolic acid in the (A) TB/HSPC/BA, (B) TB/HSPC/OA, (C) TE/HSPC/BA, and (D) TE/HSPC/OA mixed monolayer systems. The lipid mixture was component 1 [2:2:1 (m/m/m)], and ursolic acid was component 2. The mole percents of ursolic acid with respect to the lipid mixture were 0, 2.5, 5, 10, 30, 50, 70, and 100 at surface pressures of (○) 5, (△) 10, (▽) 15, (◇) 20, (left-pointing triangles) 25, and (right-pointing triangles) 30 mN m<sup>-1</sup>. The temperature was 25 °C.

Negative deviations from the ideality for  $A_{\text{ex}}$  values were recorded for all the lipids and for all mole percents of UA in the entire studied surface pressure range, which indicate attractive interactions among the components. The magnitudes of the negative deviations were higher for the unsaturated lipid (TE) than for the saturated lipid (TB), indicating better incorporation of UA into the mixed monolayer containing unsaturated lipids.

The excess free energy that determines the degree of deviation from the ideally mixed monolayer was calculated using the following expression:<sup>50</sup>

$$\Delta G_{\text{ex}}^{\circ} = \int_0^{\pi} [A - (x_1 A_1 + x_2 A_2)] d\pi \quad (6)$$

Changes in the free energy of mixing determine the thermodynamic stability of the monolayers. It can be computed from the excess free energy and the ideal free energy ( $\Delta G_{\text{id}}$ ) using eqs 7 and 8:<sup>50</sup>

$$\Delta G_{\text{mix}} = \Delta G_{\text{ex}} + \Delta G_{\text{id}} \quad (7)$$

where the ideal free energy ( $\Delta G_{\text{id}}$ ) is given by

$$\Delta G_{\text{id}} = RT(x_1 \ln x_1 + x_2 \ln x_2) \quad (8)$$

where  $R$  is the universal gas constant and  $T$  is the absolute temperature. Negative  $\Delta G_{\text{ex}}$  values, as shown in Figure 4,

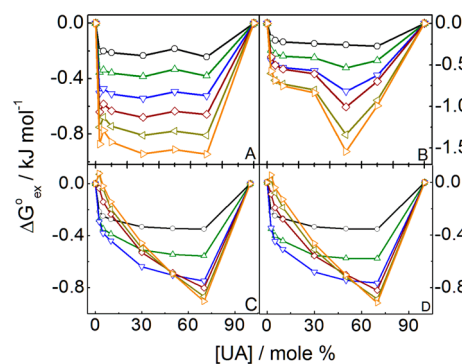


**Figure 4.** Dependence of the change in excess free energy ( $\Delta G_{\text{ex}}^{\circ}$ ) on the relative proportion of ursolic acid in the (A) TB/HSPC/BA, (B) TB/HSPC/OA, (C) TE/HSPC/BA, and (D) TE/HSPC/OA mixed monolayer systems. The lipid mixture was component 1 [2:2:1 (m/m/m)], and ursolic acid was component 2. The mole percents of ursolic acid with respect to the lipid mixture were 0, 2.5, 5, 10, 30, 50, 70, and 100 at surface pressures of (○) 5, (△) 10, (▽) 15, (◇) 20, (left-pointing triangles) 25, and (right-pointing triangles) 30 mN m<sup>-1</sup>. The temperature was 25 °C.

indicate spontaneity in the mixing processes between the components.<sup>47,50–52</sup>  $\Delta G_{\text{ex}}$  values were more negative at higher surface pressures. The minimal  $\Delta G_{\text{ex}}$  value was identified at 19, 52, 67, and 69 mol % UA for TB/HSPC/BA, TB/HSPC/OA, TE/HSPC/BA, and TE/HSPC/OA mixtures, respectively, at a  $\pi$  of 10 mN/m. These compositions, therefore, correspond to the most stable lipid/UA mixed films. The surface pressure increase in the loose packing density regimes,  $\pi \leq 10$  mN/m (LE and LE/LC phase transitions), caused the  $\Delta G_{\text{ex}}$  values of all the lipid mixtures to become more negative, because of the increase in the level of intermolecular attractive van der Waals forces.

The decrease in the  $\Delta G_{\text{ex}}$  with an increasing mole percent of UA indicates the dependence of the packing of lipid molecules on the relative proportion of UA. A negative  $\Delta G_{\text{mix}}$  value implies spontaneity in the mixing processes and strong interactions between the interfacial components, as shown in Figure S2. Negative  $\Delta G_{\text{mix}}$  values were observed at all surface pressures, thus suggesting spontaneous mutual miscibility among the components. The minimal  $\Delta G_{\text{mix}}$  value was obtained at 50 mol % UA and a surface pressure of 10 mN m<sup>-1</sup>, corresponding to the composition of the monolayer with the maximal thermodynamic stability.

The dipole moment of the film-forming materials and the change in orientation of head or tail groups in the lipid monolayer as well as of the water molecules in the subphase

**Table 1.** Mean Sizes ( $d_h$ ), PDIs,  $\zeta$  Potentials, Entrapment Efficiencies (EE%), and Loading Capacities (LC%) of Empty and Ursolic Acid-Loaded NLCs<sup>a</sup>

formulation	[UA] (mM)	size (nm)	PDI	ZP (mV)	EE%	LC%
TB/HSPC/BA	0.000	207 ± 2	0.34 ± 0.01	-16 ± 0.4		
	0.125	208 ± 1	0.34 ± 0.009	-17 ± 0.6	78.38 ± 1.9	3.78 ± 0.04
	0.250	210 ± 3	0.35 ± 0.001	-17 ± 0.5	83.55 ± 1.3	3.99 ± 0.09
	0.500	235 ± 5	0.37 ± 0.003	-18 ± 0.4	83.63 ± 0.8	3.99 ± 0.03
TB/HSPC/OA	0.000	196 ± 3	0.38 ± 0.013	-19 ± 0.8		
	0.125	184 ± 5	0.38 ± 0.009	-15 ± 0.7	80.08 ± 0.9	3.88 ± 0.03
	0.250	190 ± 7	0.38 ± 0.006	-17 ± 0.5	85.33 ± 1.5	4.09 ± 0.07
	0.500	191 ± 4	0.40 ± 0.012	-18 ± 0.1	85.56 ± 1.7	4.09 ± 0.04
TE/HSPC/BA	0.000	174 ± 2	0.34 ± 0.009	-19 ± 0.4		
	0.125	183 ± 3	0.35 ± 0.013	-19 ± 0.3	92.97 ± 1.9	4.42 ± 0.07
	0.250	191 ± 7	0.35 ± 0.024	-18 ± 0.7	94.05 ± 1.5	4.53 ± 0.02
	0.500	180 ± 2	0.35 ± 0.005	-18 ± 0.2	94.36 ± 1.7	4.59 ± 0.06
TE/HSPC/OA	0.000	147 ± 5	0.31 ± 0.016	-20 ± 0.2		
	0.125	171 ± 3	0.34 ± 0.009	-20 ± 0.4	97.14 ± 1.8	4.67 ± 0.09
	0.250	185 ± 7	0.35 ± 0.023	-20 ± 0.5	99.92 ± 1.3	4.76 ± 0.07
	0.500	182 ± 4	0.31 ± 0.008	-19 ± 0.3	99.38 ± 1.5	4.76 ± 0.02

<sup>a</sup> $N = 3$  (mean ± SD). Abbreviations: HSPC, hydrogenated soy phosphatidylcholine (common in all the systems); TB, tribehenin; TE, trierucin; BA, behenic acid; OA, oleic acid; LC, loading capacity. Drug concentrations of 0.125, 0.25, and 0.5 mM.

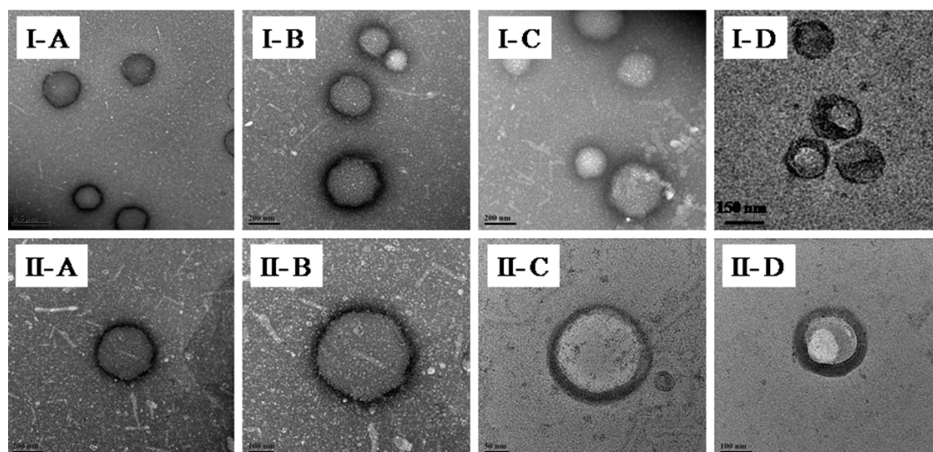


**Figure 5.** TEM images of (A) TB/HSPC/BA, (B) TB/HSPC/OA, (C) TE/HSPC/BA, and (D) TE/HSPC/OA NLC formulations. I and II denote blank NLCs and ursolic acid-loaded NLCs, respectively.

during compression give the value of surface potential. The surface potential-area measurements have been obtained to gain information about the orientation of the film constituents. Surface potential isotherms of pure components are shown in Figure S3; the formation of mixed lipid monolayers on a subphase containing pure water with and without varying concentrations of UA is shown in Figure S4. The surface potential-area profiles were more or less similar to the surface pressure-area isotherms, further supporting the aforementioned propositions.

**Dispersions and Solution Behavior of the NLCs.** *Dynamic Light Scattering (DLS) Studies.* The hydrodynamic diameter ( $d_h$ ), polydispersity index (PDI), and  $\zeta$  potential (ZP) are some of the markers of colloidal dispersion determining its stability as well as giving insight into the *in vivo* performance of NLCs. NLCs comprising triglyceride, phospholipid, and fatty acids were TB/HSPC/BA, TB/HSPC/OA, TE/HSPC/BA, and TE/HSPC/OA mixtures. The TB/TE:HSPC:BA/OA molar ratio was kept fixed at 2:2:1; the overall lipid concentration was 5 mM dispersed in 10 mM aqueous Tween 80. The size of NLCs ranged from 140 to 230 nm

with unimodal distributions. NLC formulations were studied up to 100 days (Figure S5). Particles were found to be fairly monodisperse, as revealed from the size distribution curves (data not shown) as well as from the PDI values (Figure S6). The sizes of TB/HSPC/BA, TB/HSPC/OA, TE/HSPC/BA, and TE/HSPC/OA NLCs were found to be  $220 \pm 8$ ,  $190 \pm 7$ ,  $174 \pm 4$ , and  $147 \pm 5$  nm, respectively, with size increasing in the following order: TE/HSPC/OA < TE/HSPC/BA < TB/HSPC/OA < TB/HSPC/BA [where the percentages of unsaturation in the fatty acyl hydrocarbon chains were 60, 40, 20, and 0, respectively (Table 1)]. Stronger association among the lipidic components in the case of unsaturated lipid and fatty acid resulted in size constriction compared to that in the saturated lipids.<sup>53,54</sup> The DLS results thus could be correlated with the monolayer studies; the extents of negative deviation from ideality were higher among fluid lipids. An increasing amount of UA increased the size of TB/HSPC/BA and TE/HSPC/BA NLCs (Figure S5A,C). The lower multicrystallinity in the case of the lipid systems with lower degrees of unsaturation restricts the drug molecules mostly to reside on the palisade layer of the NLC, which subsequently results in the

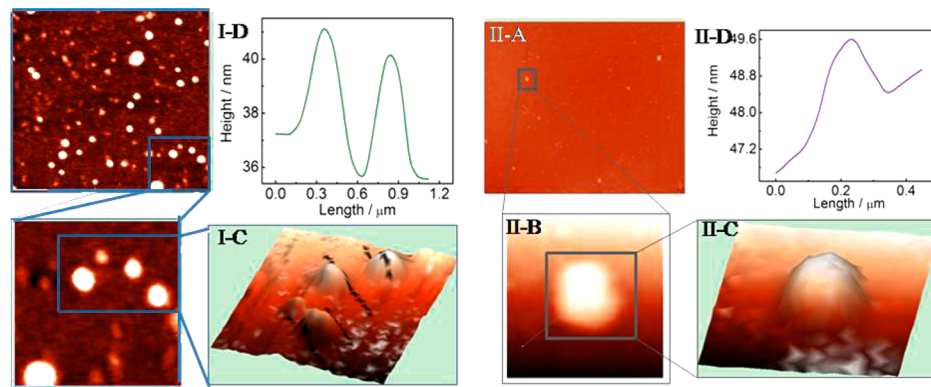


**Figure 6.** Representative AFM images of (I) TB/HSPC/BA and (II) TE/HSPC/OA NLC formulations. (A and B) Two-dimensional images, (C) three-dimensional images, and (D) section analysis.

swelling of the NLC leading to an increase in  $d_h$ . On the other hand, in the case of more fluidic combinations (TB/HSPC/OA and TE/HSPC/OA), there was an initial increase in size with the addition of drug; the effect became insignificant with size variation at higher drug concentrations (Figure SSB,D).

Better incorporation and drug solubilization in the case of liquid lipids direct the drug to the core of the NLC, resulting in a significant influence of the added drug on  $d_h$ . In all cases, the size of the NLC formulations increased with time probably because of the tendency of the NLC formulations to coagulate. PDI values of <0.5 indicate homogeneity of the NLC formulation (Figure S6). A negative ZP was due to the dissociation of fatty acid in NLCs (Figure S7). The extent of dissociation of the incorporated fatty acid was higher for fluid lipids, for which negative values of ZP were recorded. In addition, the liquid lipid reduced  $d_h$  and consequently decreased the effective NLC surface area; thus, the ZP values for the systems having larger amounts of liquid lipids were higher. The effect of UA on the ZP of NLCs was not significant because of its nonionic nature. In all cases, the magnitude of ZP decreased with storage time (Figure S7), which was due to the structural modification of lipidic components as well as the Ostwald ripening/coagulation process, common for colloidal dispersions.<sup>55</sup>

**Morphological Studies.** The size of NLCs, as evaluated from TEM studies (Figure 5), could be well correlated with particle size as determined by DLS measurements. NLCs were spherical with a smooth surface in the case of TB/HSPC/BA and TB/HSPC/OA formulations. While good contrast and distinct images were visualized in the former category, however, in the case of TE/HSPC/BA and TE/HSPC/OA formulations, contrast and distinctness were somehow reduced. It might be due to the presence of a larger amount of liquid lipid in the NLC formulation. The existence of individual and distinct particles also indicates the monodisperse nature of the formulations, as was also observed by DLS.<sup>56,57</sup>

Representative AFM images of TB/HSPC/BA and TE/HSPC/OA NLCs are shown in Figure 6. NLCs were found to be spherical with a smooth surface. NLCs were separated from each other, indicating the absence of aggregated species. The observed particle sizes (200–230 nm) were comparable to those of the DLS and TEM studies. The particles were very distinct (Figure 6, II-A and II-B), unlike TE/HSPC/OA NLCs, whose size was found to be in the range of 160–200 nm, with less contrast and distinctiveness. The TB/HSPC/BA and TE/HSPC/OA NLC systems showed the observed vertical

dimension to be as large as 4.1 and 2.9 nm, respectively. This could be explained by the presence of larger amounts of unsaturated lipid in the second category of NLCs than in the former.

**Differential Scanning Calorimetric (DSC) Studies.** Phase transition temperatures ( $T_m$ ) of tribehenin, trierucin, behenic acid, oleic acid, hydrogenated soy phosphatidylcholine, and the drug ursolic acid were found to be 82.9, 30.1, 81.4, 14.3, and 283.7 °C, respectively, as shown in Figure S8. The main rationale of this study was to perceive whether the crystallinity differed in the lipid matrices due to the presence of saturation and unsaturation in their mixed states in the form of NLCs. In case of the physical mixtures (where the components were dissolved in organic solvents and subsequently dried under vacuum), the sharp peak of UA, which appeared at 283.7 °C in its pure state, disappeared (data not shown).

This indicates complete solubilization of the amorphous state of ursolic acid in the lipid matrix.<sup>58</sup> The thermal behavior of the physical mixture of lipids and UA with lipids was also assessed (Figure S9).  $T_m$  values of the TB/HSPC/BA, TB/HSPC/OA, TB/HSPC/BA/UA, and TB/HSPC/OA/UA physical mixtures appeared at 80.1, 80.4, 77.5, and 77.8 °C, respectively (Figure S9A).  $T_m$  values of the TE/HSPC/BA, TE/HSPC/OA, TE/HSPC/BA/UA, and TE/HSPC/OA/UA physical mixtures were 27.9, 19.6, 27.8, and 20.0 °C, respectively (Figure S9B). Table 2 describes the combined thermodynamic parameters, derived from the DSC thermograms. The  $T_m$  value of the UA/lipid mixture, however, decreased significantly upon loading of UA into saturated lipid, which indicates a decrease in the crystallinity of the lipid matrix; this may be attributed to UA entrapment in the case of NLCs. On the other hand, the  $T_m$  values of the UA/lipid mixture did not change much with loading of UA into unsaturated lipid, although the peak was broader compared to that of the corresponding physical mixture of lipid, which may be attributed to the entrapment of UA in the NLCs. The endothermic and exothermic peaks of the physical mixtures of TB/HSPC/OA NLCs were shifted from 80 to 64 °C and from 30 to 32 °C, respectively, in the presence of UA (Figure S10). This shift was a combined effect of the inclusion of Tween 80 (on the palisade layer) as well as the drug into the core of NLCs. The endothermic peaks were taken into account to derive other associated thermal parameters, viz., changes in enthalpy ( $\Delta H$ ), heat capacity ( $\Delta C_p$ ), and width of the melting peak at half-maxima ( $\Delta T_{1/2}$ ). DSC heating curves of different lipid matrices, viz., TB/HSPC/

**Table 2. Temperatures for Maximal Heat Flow ( $T_m$ ), Widths at Half-Peak Height ( $\Delta T_{1/2}$ ), and Changes in Enthalpy ( $\Delta H$ ) and Heat Capacity ( $\Delta C_p$ ) of Blank and UA-Loaded NLCs**

formulation	[UA] (mM)	$T_m$ (°C)	$\Delta T_{1/2}$ (°C)	$\Delta H$ (kcal mol <sup>-1</sup> )	$\Delta C_p$ (kcal mol <sup>-1</sup> C <sup>-1</sup> )
TB/HSPC/ BA	0.000	30.0	2.5	1.49	0.61
	0.125	35.4	2.5	1.81	0.71
	0.250	34.7	2.7	2.62	0.96
	0.500	34.5	2.9	3.72	1.28
TB/HSPC/ OA	0.000	29.7	4.9	1.22	0.25
	0.125	30.0	6.6	4.42	0.67
	0.250	29.1	6.9	2.40	0.35
	0.500	26.6	7.5	1.61	0.22
TE/HSPC/ BA	0.000	8.0	3.0	1.93	0.65
	0.125	8.6	3.2	3.39	1.06
	0.250	5.9	3.4	7.97	2.32
	0.500	4.0	4.4	9.79	2.21
TE/HSPC/ OA	0.000	2.2	4.9	1.92	0.39
	0.125	4.0	5.3	2.55	0.49
	0.250	3.9	5.6	2.55	0.45
	0.500	3.7	5.8	2.52	0.43

BA, TB/HSPC/OA, TE/HSPC/BA, and TE/HSPC/OA NLCs, in the presence and absence of UA are given in Figure 7.

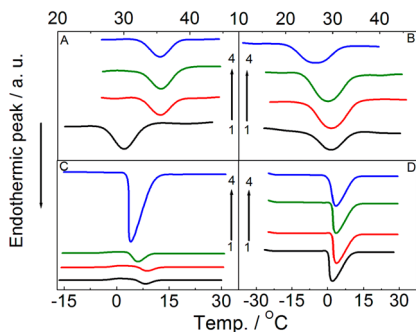


**Figure 7.** DSC heating curves of ursolic acid-loaded NLCs: (A) TB/HSPC/BA, (B) TB/HSPC/OA, (C) TE/HSPC/BA, and (D) TE/HSPC/OA. Ursolic acid concentrations of (1) 0, (2) 0.125, (3) 0.25, and (4) 0.5 mM. The scan rate was 2.5 °C/min.

Considering the drug free systems, significant changes in the  $T_m$  values were noted between saturated and unsaturated lipids as well as fatty acids. The  $T_m$  values were 80.1 and 80.4 °C for TB/HSPC/BA and TB/HSPC/OA formulations, respectively, but were 27.9 and 19.6 °C for TE/HSPC/BA and TE/HSPC/OA formulations, respectively. The decrease in  $T_m$  with a decrease in the size of NLCs could be explained by the Thomson proposition.<sup>43</sup> It has already been observed from the DLS studies that the NLCs formulated by saturated lipid and fatty acid were larger than the NLCs comprising unsaturated lipid and fatty acid. It is not unexpected that the smaller entities would have melting temperatures lower than those of the larger particles.

In the case of TE/HSPC/OA and TB/HSPC/BA NLCs, the phase transition temperature passed through maxima with an increasing UA concentration. These results indicate that at lower concentrations the drug molecules reside on the surface

of NLCs and at higher concentrations the drug molecules are partitioned into the NLC core. In case of TE/HSPC/BA and TB/HSPC/OA NLCs, a progressive decrease in the phase transition temperature was observed with an increase in drug concentration. Increased multicrystallinity, contributed by the added drug, reduces the lowering of phase transition temperature. The liquid lipids further help the drug molecules become introduced into the core and enhance the multicrystallinity, as further supported by the increasing  $\Delta T_{1/2}$  with increasing UA concentration. Incorporation of UA also increases  $\Delta H$  and  $\Delta C_p$ . The higher multicrystallinity led to the formation of aggregated clusters; consequently,  $\Delta H$  and  $\Delta C_p$  increase. In the case of TB/HSPC/OA NLCs, the extent of cluster formulation is lower because of the rigidity of NLCs. Hence, significant enhancement of the phase transition enthalpy and heat capacity was observed at the higher drug concentration for the said NLC formulation.

**Determination of UA Entrapment Efficiency and Drug Loading Capacity.** Entrapment efficiency (EE) and drug loading (DL) capacity values, to estimate the quantity of UA incorporated into the NLCs, are summarized in Table 1 along with other data. The entrapment efficiency decreased in the following order: TE/HSPC/OA > TE/HSPC/BA > TB/HSPC/OA > TB/HSPC/BA (in accordance with the lipophilicity and stronger associative interaction between drugs and lipid molecules). Incorporation of the liquid fatty acid into solid lipids causes a reduction in crystallinity, consequently resulting in more imperfections in the lipid matrix and providing more space for UA molecules.<sup>16,54,59,60</sup> Thus, the proposition of the DSC studies was further supported by such results. The entrapment efficiency and drug loading results are well correlated with monolayer studies. With an increasing concentration of UA, a marked increase in the percentage of encapsulated drug up to 0.25 mM was recorded, beyond which it did not change appreciably.

**In Vitro Release Kinetics for Release of Ursolic Acid from NLCs.** The cumulative percentage releases of UA from NLC dispersions over 96 h are shown in Figure 8.

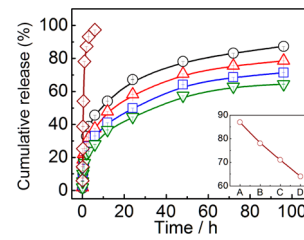


**Figure 8.** *In vitro* cumulative release of ursolic acid from NLCs. Composition of NLCs: (green triangles) TB/HSPC/BA, (blue squares) TB/HSPC/OA, (red triangles) TE/HSPC/BA, (black circles) TE/HSPC/OA, and (maroon diamonds) free UA in PBS (pH 7.4) and 1% (v/v) Tween 80 at 37 ± 0.1 °C. Error bars represent the standard deviation (SD) of three different release experiments.

Values for the release of UA from the TE/HSPC/OA, TE/HSPC/BA, TB/HSPC/OA, and TB/HSPC/BA formulations of 87, 78, 71, and 64%, respectively, were recorded, as presented in the inset of Figure 8. The release of UA from NLC was dependent on NLC composition.<sup>61</sup> A larger amount of UA was released from the unsaturated lipid blends than from the blends of saturated lipids.<sup>62</sup> Native UA (without any NLC, control) showed more rapid release than UA-loaded NLC, indicating sustained release of UA incorporated into NLC

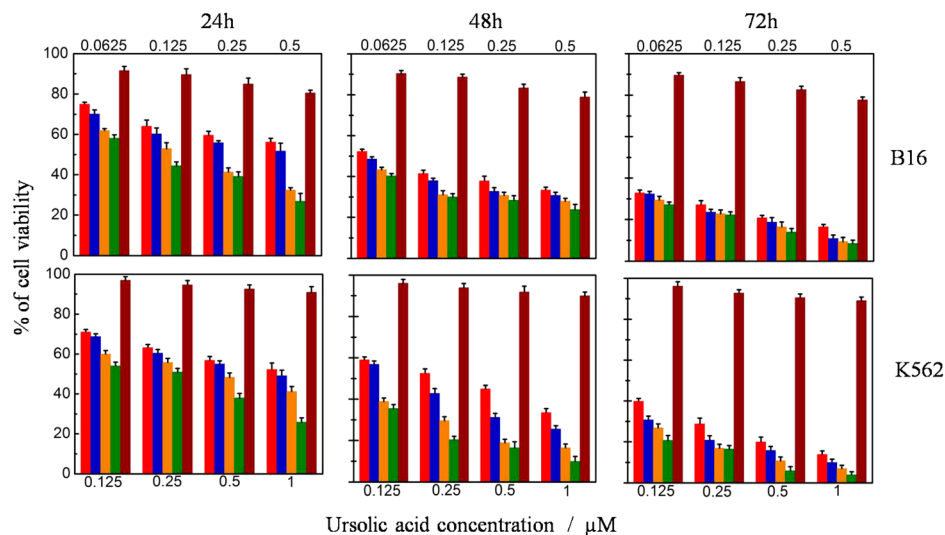


**Figure 9.** *In vitro* cytotoxicity activity of free ursolic acid (brown) and ursolic acid loaded with different NLCs, TB/HSPC/BA (red), TB/HSPC/OA (blue), TE/HSPC/BA (orange), and TE/HSPC/OA (green), on the viability of B16 and K562 cells. Cells were grown and treated for 24, 48, and 72 h. Experiments were performed in triplicate, with the results showing the mean and standard deviation of the triplicate of each group. The experiments were repeated three times with similar results.

compared to that of native UA. Thus, the NLC dispersion could be a useful carrier with better control of UA release.

The two-step release was observed for UA loaded in all NLCs, as evidenced by the initial burst release within 3 h (39, 31, 26, and 23%) followed by a sustained release up to 96 h (87, 79, 71, and 64%). This could account for the fact that the drug encapsulation efficiency in these NLCs (i.e., matrix type or reservoir type) and surface properties both could affect the release behavior of UA-loaded NLCs.<sup>16</sup> The initial burst release can be explained on the basis of the release of UA enriched in the outer shell of NLCs.

**In Vitro Cytotoxicity Studies.** *In vitro* cytotoxicity assays were conducted on human melanoma cell line B16 and leukemic cell line K562 by performing the MTT assay for UA upon administration in free forms or loaded in different NLCs, as shown in Figure 9. Blank NLCs did not show any significant cytotoxicity.

IC<sub>50</sub> values at 24 h for free UA and UA loaded in TE/HSPC/OA and TE/HSPC/BA NLCs were 7.7, 0.041, and 0.10 μM for the B16 cell line and 224.38, 0.14, and 0.23 μM for the K562 cell line, respectively. However, the IC<sub>50</sub> values of UA at 48 h when it is loaded in TB/HSPC/OA and TB/HSPC/BA NLCs were 0.062, 0.052, 0.09, and 0.19 μM for B16 and K562 cell lines, respectively. Lower IC<sub>50</sub> values of UA-loaded NLCs, compared to that of free UA, suggest superior activity of the drug-loaded NLC compared to that of the free drug. Cytotoxicities of different UA-loaded NLCs comprising lipid matrices are also important attributes because UA loaded in TE/HSPC/OA and TE/HSPC/BA NLCs showed cytotoxicity higher than that in TB/HSPC/OA and TB/HSPC/BA NLCs in terms of concentration of UA and incubation time. The minimal IC<sub>50</sub> values, lower incubation times, and higher cytotoxicities for TE/HSPC/OA and TE/HSPC/BA NLCs against both the cell lines could be attributed to the fact that the higher encapsulation efficiency, faster release, and smaller size of the unsaturated lipid led to better internalization of the drug into the cell.

Furthermore, the capability of the formulations increased when either the concentration of UA-loaded NLCs was

increased or the incubation time was extended for UA-loaded NLCs. The results indicated that the anticancer activity of UA against both types of cells occurred in a concentration- and time-dependent manner. This dominance may mainly be caused by better internalization of the UA-loaded NLCs and the sustained release of UA inside the cancer cells.<sup>32</sup> It is worth mentioning that UA-loaded NLCs showed remarkable anticancer activities against K562 cells, which is otherwise a multidrug resistant cell line. UA-loaded NLCs thus hold the promise of overcoming multidrug resistance, and this aspect should be extensively exploited in cancer treatment.

## CONCLUSIONS

In this study, NLCs comprising saturated and unsaturated lipids and containing pentacyclic triterpenoid ursolic acid were successfully formulated. The findings reveal the influence of saturated and unsaturated lipids and fatty acids on the particle size, polydispersity index,  $\zeta$  potential, drug encapsulation efficiency, *in vitro* release behavior, and *in vitro* cytotoxicity of the formulation. The studies of surface pressure ( $\pi$ )–area (A) isotherms of pure components, mixed lipids, and mixed lipids with ursolic acid suggest that ursolic acid alters the interfacial organization of lipids. The spherical morphology of NLCs with a smooth surface was observed for all the formulations. Significant differences in crystal structure between NLCs comprising saturated and unsaturated lipids were noted, whereby the crystallinity of UA was lost because of its incorporation into the NLCs. Release of the drug was sustained for all the NLCs; unsaturated lipids exhibited drug release faster than that of saturated components. The most useful finding from this report is the significant difference between the cytotoxicity of free UA and UA-loaded NLCs, which demonstrates the superiority of UA-loaded NLCs over free UA in penetrating the cell membrane. UA in saturated and unsaturated lipids and fatty acid comprising NLCs showed comparable cytotoxicity in human leukemic cell line K562 and melanoma cell line B16 and enhanced anticancer activity. Conclusively, both saturated and unsaturated lipid-containing

NLCs formulated in this study may be used as potential delivery systems for UA with improved anticancer activity.

## ■ ASSOCIATED CONTENT

### Supporting Information

The Supporting Information is available free of charge on the ACS Publications website at DOI: [10.1021/acs.langmuir.6b02402](https://doi.org/10.1021/acs.langmuir.6b02402).

Additional findings ([PDF](#))

## ■ AUTHOR INFORMATION

### Corresponding Author

\*Department of Chemistry and Chemical Technology, Vidyasagar University, Midnapore 721 102, West Bengal, India. E-mail: [akpanda@mail.vidyasagar.ac.in](mailto:akpanda@mail.vidyasagar.ac.in). Phone: +919433347210. Fax: +91322275329/297.

### Notes

The authors declare no competing financial interest.

## ■ ACKNOWLEDGMENTS

Financial support in the form of a research grant (SR/S1/PC/32/2011) from the Department of Science and Technology, Government of India, New Delhi, is sincerely acknowledged. P.N. acknowledges the receipt of a research fellowship from the University Grant Commission, New Delhi, under the Rajiv Gandhi National Fellowship for the disabled (F./2012-13/RGNF-2012-13D-GENCHH-51106/31-Oct-2013). B.A.N. and A.K.P. sincerely acknowledge the support from the Indo-Russian Collaborative research project, funded by the Department of Science and Technology, Government of India (Project INT/RUS/RFBR/P-220), and the Russian Foundation of Basic Research (RFBR № 15-53-45043\_IND\_a). A.G.B., A.V.A., and B.A.N. acknowledge St. Petersburg State University for Research Grant 12.38.241.2014. P.N. sincerely acknowledges the valuable guidance from Dr. B. Achari of the CSIR-Indian Institute of Chemical Biology, Kolkata, India.

## ■ REFERENCES

- (1) Baird, R. D.; Kaye, S. B. Drug resistance reversal—are we getting closer? *Eur. J. Cancer* **2003**, *39* (17), 2450–61.
- (2) Gieseler, F.; Rudolph, P.; Kloeppe, G.; Foelsch, U. R. Resistance mechanisms of gastrointestinal cancers: why does conventional chemotherapy fail? *Int. J. Colorectal Dis.* **2003**, *18* (6), 470–80.
- (3) Schilsky, R. L.; Milano, G. A.; Ratain, M. J. *Principles of Antineoplastic Drug Development and Pharmacology*; Taylor & Francis: New York, 1996; pp 457–486.
- (4) Junyaprasert, V. B.; Morakul, B. Nanocrystals for enhancement of oral bioavailability of poorly water-soluble drugs. *Asian J. Pharm. Sci.* **2015**, *10* (1), 13–23.
- (5) Khadka, P.; Ro, J.; Kim, H.; Kim, I.; Kim, J. T.; Kim, H.; Cho, J. M.; Yun, G.; Lee, J. Pharmaceutical particle technologies: An approach to improve drug solubility, dissolution and bioavailability. *Asian J. Pharm. Sci.* **2014**, *9* (6), 304–316.
- (6) Müller, R.; Petersen, R.; Hommoss, A.; Pardeike, J. Nanostructured lipid carriers (NLC) in cosmetic dermal products. *Adv. Drug Delivery Rev.* **2007**, *59* (6), 522–530.
- (7) Dang, H.; Meng, M. H. W.; Zhao, H.; Iqbal, J.; Dai, R.; Deng, Y.; Lv, F. Luteolin-loaded solid lipid nanoparticles synthesis, characterization, & improvement of bioavailability, pharmacokinetics in vitro and vivo studies. *J. Nanopart. Res.* **2014**, *16* (4), 2347.
- (8) Gaur, P. K.; Mishra, S.; Bajpai, M.; Mishra, A. Enhanced Oral Bioavailability of Efavirenz by Solid Lipid Nanoparticles: In Vitro Drug Release and Pharmacokinetics Studies. *BioMed Res. Int.* **2014**, *2014*, 9.
- (9) Kaur, I. P.; Bhandari, R.; Bhandari, S.; Kakkar, V. Potential of solid lipid nanoparticles in brain targeting. *J. Controlled Release* **2008**, *127* (2), 97–109.
- (10) Mehnert, W.; Mäder, K. Solid lipid nanoparticles: production, characterization and applications. *Adv. Drug Delivery Rev.* **2001**, *47* (2), 165–196.
- (11) Wong, H. L.; Bendayan, R.; Rauth, A. M.; Li, Y.; Wu, X. Y. Chemotherapy with anticancer drugs encapsulated in solid lipid nanoparticles. *Adv. Drug Delivery Rev.* **2007**, *59* (6), 491–504.
- (12) Hu, F.-Q.; Jiang, S.-P.; Du, Y.-Z.; Yuan, H.; Ye, Y.-Q.; Zeng, S. Preparation and characteristics of monostearin nanostructured lipid carriers. *Int. J. Pharm.* **2006**, *314* (1), 83–89.
- (13) Shen, J.; Sun, M.; Ping, Q.; Ying, Z.; Liu, W. Incorporation of liquid lipid in lipid nanoparticles for ocular drug delivery enhancement. *Nanotechnology* **2010**, *21* (2), 025101.
- (14) Pardeike, J.; Weber, S.; Haber, T.; Wagner, J.; Zarfl, H. P.; Plank, H.; Zimmer, A. Development of an Itraconazole-loaded nanostructured lipid carrier (NLC) formulation for pulmonary application. *Int. J. Pharm.* **2011**, *419* (1–2), 329–338.
- (15) Teeranachaideekul, V.; Souto, E. B.; Junyaprasert, V. B.; Müller, R. H. Cetyl palmitate-based NLC for topical delivery of Coenzyme Q 10—Development, physicochemical characterization and in vitro release studies. *Eur. J. Pharm. Biopharm.* **2007**, *67* (1), 141–148.
- (16) Souto, E. B.; Wissing, S. A.; Barbosa, C. M.; Müller, R. H. Development of a controlled release formulation based on SLN and NLC for topical clotrimazole delivery. *Int. J. Pharm.* **2004**, *278* (1), 71–77.
- (17) Yuan, H.; Wang, L.-L.; Du, Y.-Z.; You, J.; Hu, F.-Q.; Zeng, S. Preparation and characteristics of nanostructured lipid carriers for control-releasing progesterone by melt-emulsification. *Colloids Surf., B* **2007**, *60* (2), 174–179.
- (18) Goutayer, M.; Dufort, S.; Josserand, V.; Royère, A.; Heinrich, E.; Vinet, F.; Bibette, J.; Coll, J.-L.; Texier, I. Tumor targeting of functionalized lipid nanoparticles: assessment by in vivo fluorescence imaging. *Eur. J. Pharm. Biopharm.* **2010**, *75* (2), 137–147.
- (19) Teskač, K.; Kristl, J. The evidence for solid lipid nanoparticles mediated cell uptake of resveratrol. *Int. J. Pharm.* **2010**, *390* (1), 61–69.
- (20) Yuan, H.; Miao, J.; Du, Y.-Z.; You, J.; Hu, F.-Q.; Zeng, S. Cellular uptake of solid lipid nanoparticles and cytotoxicity of encapsulated paclitaxel in A549 cancer cells. *Int. J. Pharm.* **2008**, *348* (1–2), 137–145.
- (21) Chen, C.-C.; Tsai, T.-H.; Huang, Z.-R.; Fang, J.-Y. Effects of lipophilic emulsifiers on the oral administration of lovastatin from nanostructured lipid carriers: physicochemical characterization and pharmacokinetics. *Eur. J. Pharm. Biopharm.* **2010**, *74* (3), 474–482.
- (22) Müller, R.; Radtke, M.; Wissing, S. Nanostructured lipid matrices for improved microencapsulation of drugs. *Int. J. Pharm.* **2002**, *242* (1), 121–128.
- (23) Teeranachaideekul, V.; Müller, R. H.; Junyaprasert, V. B. Encapsulation of ascorbyl palmitate in nanostructured lipid carriers (NLC)—effects of formulation parameters on physicochemical stability. *Int. J. Pharm.* **2007**, *340* (1), 198–206.
- (24) Laszczyk, M. N. Pentacyclic triterpenes of the lupane, oleanane and ursane group as tools in cancer therapy. *Planta Med.* **2009**, *75* (15), 1549–60.
- (25) Checker, R.; Sandur, S. K.; Sharma, D.; Patwardhan, R. S.; Jayakumar, S.; Kohli, V.; Sethi, G.; Aggarwal, B. B.; Sainis, K. B. Potent anti-inflammatory activity of ursolic acid, a triterpenoid antioxidant, is mediated through suppression of NF-κB, AP-1 and NF-AT. *PLoS One* **2012**, *7* (2), e31318.
- (26) Chiang, L.; Chiang, W.; Chang, M.; Ng, L.; Lin, C. Antiviral activity of *Plantago major* extracts and related compounds in vitro. *Antiviral Res.* **2002**, *55* (1), 53–62.
- (27) Chung, P. Y.; Navaratnam, P.; Chung, L. Y. Synergistic antimicrobial activity between pentacyclic triterpenoids and antibiotics against *Staphylococcus aureus* strains. *Ann. Clin. Microbiol. Antimicrob.* **2011**, *10* (1), 25.

- (28) Saravanan, R.; Viswanathan, P.; Pugalendi, K. V. Protective effect of ursolic acid on ethanol-mediated experimental liver damage in rats. *Life Sci.* **2006**, *78* (7), 713–718.
- (29) Yan, S.-l.; Huang, C.-y.; Wu, S.-t.; Yin, M. -c., Oleanolic acid and ursolic acid induce apoptosis in four human liver cancer cell lines. *Toxicol. In Vitro* **2010**, *24* (3), 842–848.
- (30) Caldeira de Araújo Lopes, S.; Vinícius Melo Novais, M.; Salviano Teixeira, C.; Honorato-Sampaio, K.; Tadeu Pereira, M.; Ferreira, L. A. M.; Braga, F. C.; Oliveira, M. C. Preparation, Physicochemical Characterization, and Cell Viability Evaluation of Long-Circulating and pH-Sensitive Liposomes Containing Ursolic Acid. *BioMed Res. Int.* **2013**, *2013*, 7.
- (31) Song, J.; Wang, Y.; Song, Y.; Chan, H.; Bi, C.; Yang, X.; Yan, R.; Wang, Y.; Zheng, Y. Development and characterisation of ursolic acid nanocrystals without stabiliser having improved dissolution rate and in vitro anticancer activity. *AAPS PharmSciTech* **2014**, *15* (1), 11–19.
- (32) Zhang, H.; Li, X.; Ding, J.; Xu, H.; Dai, X.; Hou, Z.; Zhang, K.; Sun, K.; Sun, W. Delivery of ursolic acid (UA) in polymeric nanoparticles effectively promotes the apoptosis of gastric cancer cells through enhanced inhibition of cyclooxygenase 2 (COX-2). *Int. J. Pharm.* **2013**, *441* (1–2), 261–8.
- (33) Zhang, H.; Zheng, D.; Ding, J.; Xu, H.; Li, X.; Sun, W. Efficient delivery of ursolic acid by poly(N-vinylpyrrolidone)-block-poly ( $\epsilon$ -caprolactone) nanoparticles for inhibiting the growth of hepatocellular carcinoma in vitro and in vivo. *Int. J. Nanomed.* **2015**, *10*, 1909–1920.
- (34) Alvarado, H. L.; Abrego, G.; Garduno-Ramirez, M. L.; Clares, B.; Calpena, A. C.; Garcia, M. L. Design and optimization of oleanolic/ursolic acid-loaded nanoplatforms for ocular anti-inflammatory applications. *Nanomedicine* **2015**, *11* (3), 521–30.
- (35) Jin, H.; Pi, J.; Yang, F.; Wu, C.; Cheng, X.; Bai, H.; Huang, D.; Jiang, J.; Cai, J.; Chen, Z. W. Ursolic acid-loaded chitosan nanoparticles induce potent anti-angiogenesis in tumor. *Appl. Microbiol. Biotechnol.* **2016**, *100*, 6643–6652.
- (36) Yang, L.; Sun, Z.; Zu, Y.; Zhao, C.; Sun, X.; Zhang, Z.; Zhang, L. Physicochemical properties and oral bioavailability of ursolic acid nanoparticles using supercritical anti-solvent (SAS) process. *Food Chem.* **2012**, *132* (1), 319–325.
- (37) Mandelli Almeida, M.; Nadia, A. B.-C.; Denise, C. J.; Mary, K. T.; Rolim, B. A.; Robles, V. M. V. Evaluation of physical and chemical stability of nanostructured lipid carries containing ursolic acid in cosmetic formulation. *J. Appl. Pharm. Sci.* **2013**, *3* (3), 5–8.
- (38) Zhou, X. J.; Hu, X. M.; Yi, Y. M.; Wan, J. Preparation and body distribution of freeze-dried powder of ursolic acid phospholipid nanoparticles. *Drug Dev. Ind. Pharm.* **2009**, *35* (3), 305–10.
- (39) Lopes, S. C.; Novais, M. V.; Ferreira, D. S.; Braga, F. C.; Magalhães-Paniago, R.; Malachias, A.; Oliveira, M. C. Ursolic acid incorporation does not prevent the formation of a non-lamellar phase in pH-sensitive and long-circulating liposomes. *Langmuir* **2014**, *30* (50), 15083–15090.
- (40) de Oliveira Eloy, J.; Saraiva, J.; de Albuquerque, S.; Marchetti, J. M. Solid dispersion of ursolic acid in Gelucire 50/13: a strategy to enhance drug release and trypanocidal activity. *AAPS PharmSciTech* **2012**, *13* (4), 1436–45.
- (41) Vyas, A. Preparation and characterization of the inclusion complex of ursolic acid with polymerized hydrophilic cyclodextrin. *Planta Med.* **2015**, *81* (05), PP20.
- (42) Wei, Z.; Bi, S. M. The Preparation and Characterization of Inclusion Complex of Ursolic Acid with  $\gamma$ -Cyclodextrin. *Adv. Mater. Res.* **2011**, *403–408*, 712–716.
- (43) Nahak, P.; Karmakar, G.; Roy, B.; Guha, P.; Sapkota, M.; Koirala, S.; Chang, C.-H.; Panda, A. K. Physicochemical studies on local anaesthetic loaded second generation nanolipid carriers. *RSC Adv.* **2015**, *5* (33), 26061–26070.
- (44) Jain, A. K.; Jain, A.; Garg, N. K.; Agarwal, A.; Jain, A.; Tyagi, R. K.; Jain, S. A.; Jain, R. K.; Agrawal, H.; Agrawal, G. P. Adapalene loaded solid lipid nanoparticles gel: an effective approach for acne treatment. *Colloids Surf., B* **2014**, *121*, 222–229.
- (45) Alwarawrah, M.; Dai, J.; Huang, J. A Molecular View of the Cholesterol Condensing Effect in DOPC Lipid Bilayers. *J. Phys. Chem. B* **2010**, *114* (22), 7516–7523.
- (46) Nowotarska, S. W.; Nowotarski, K. J.; Friedman, M.; Situ, C. Effect of structure on the interactions between five natural antimicrobial compounds and phospholipids of bacterial cell membrane on model monolayers. *Molecules* **2014**, *19* (6), 7497–515.
- (47) Panda, A. K.; Nag, K.; Harbottle, R. R.; Possmayer, F.; Petersen, N. O. Thermodynamic studies on mixed molecular langmuir films: Part 2. Mutual mixing of DPPC and bovine lung surfactant extract with long-chain fatty acids. *Colloids Surf., A* **2004**, *247* (1–3), 9–17.
- (48) Yasemann, A.; Sukharev, S. Properties of Diphytanoyl Phospholipids at the Air–Water Interface. *Langmuir* **2015**, *31* (1), 350–357.
- (49) Karmakar, G.; Nahak, P.; Guha, P.; Roy, B.; Chettri, P.; Sapkota, M.; Koirala, S.; Misono, T.; Torigoe, K.; Ghosh, S.; Panda, A. K. Effects of Fatty Acids on the Interfacial and Solution Behavior of Mixed Lipidic Aggregates Called Solid Lipid Nanoparticles. *J. Oleo Sci.* **2016**, *65* (5), 419–430.
- (50) Guha, P.; Roy, B.; Karmakar, G.; Nahak, P.; Koirala, S.; Sapkota, M.; Misono, T.; Torigoe, K.; Panda, A. K. Ion-Pair Amphiphile: A Neoteric Substitute That Modulates the Physicochemical Properties of Biomimetic Membranes. *J. Phys. Chem. B* **2015**, *119* (11), 4251–4262.
- (51) Chou, T.-H.; Chang, C.-H. Thermodynamic Characteristics of Mixed DPPC/DHDP Monolayers on Water and Phosphate Buffer Subphases. *Langmuir* **2000**, *16* (7), 3385–3390.
- (52) Panda, A. K.; Nag, K.; Harbottle, R. R.; Possmayer, F.; Petersen, N. O. Thermodynamic studies of bovine lung surfactant extract mixing with cholesterol and its palmitate derivative. *J. Colloid Interface Sci.* **2007**, *311* (2), 551–555.
- (53) Fang, J.-Y.; Fang, C.-L.; Liu, C.-H.; Su, Y.-H. Lipid nanoparticles as vehicles for topical psoralen delivery: Solid lipid nanoparticles (SLN) versus nanostructured lipid carriers (NLC). *Eur. J. Pharm. Biopharm.* **2008**, *70* (2), 633–640.
- (54) Gaba, B.; Fazil, M.; Khan, S.; Ali, A.; Baboota, S.; Ali, J. Nanostructured lipid carrier system for topical delivery of terbinafine hydrochloride. *Bull. Fac. Pharm.* **2015**, *53* (2), 147–159.
- (55) Wooster, T. J.; Golding, M.; Sanguansri, P. Impact of oil type on nanoemulsion formation and Ostwald ripening stability. *Langmuir* **2008**, *24* (22), 12758–65.
- (56) Neupane, Y. R.; Srivastava, M.; Ahmad, N.; Kumar, N.; Bhatnagar, A.; Kohli, K. Lipid based nanocarrier system for the potential oral delivery of decitabine: Formulation design, characterization, ex vivo, and in vivo assessment. *Int. J. Pharm.* **2014**, *477* (1–2), 601–612.
- (57) Sütö, B.; Berkó, S.; Kozma, G.; Kukovecz, Á.; Budai-Szücs, M.; Erös, G.; Kemény, L.; Sztojkov-Ivanov, A.; Gáspar, R.; Csányi, E. Development of ibuprofen-loaded nanostructured lipid carrier-based gels: characterization and investigation of in vitro and in vivo penetration through the skin. *Int. J. Nanomed.* **2016**, *11*, 1201–1212.
- (58) Kashanian, S.; Rostami, E. PEG-stearate coated solid lipid nanoparticles as levothyroxine carriers for oral administration. *J. Nanopart. Res.* **2014**, *16* (3), 1–10.
- (59) Jenning, V.; Thunemann, A. F.; Gohla, S. H. Characterisation of a novel solid lipid nanoparticle carrier system based on binary mixtures of liquid and solid lipids. *Int. J. Pharm.* **2000**, *199* (2), 167–77.
- (60) Patel, D.; Dasgupta, S.; Dey, S.; Ramani, Y. R.; Ray, S.; Mazumder, B. Nanostructured Lipid Carriers (NLC)-Based Gel for the Topical Delivery of Aceclofenac: Preparation, Characterization, and In Vivo Evaluation. *Sci. Pharm.* **2012**, *80* (3), 749–764.
- (61) Venishetty, V. K.; Chede, R.; Komuravelli, R.; Adepu, L.; Sistla, R.; Diwan, P. V. Design and evaluation of polymer coated carvedilol loaded solid lipid nanoparticles to improve the oral bioavailability: A novel strategy to avoid intraduodenal administration. *Colloids Surf., B* **2012**, *95*, 1–9.
- (62) Carafa, M.; Santucci, E.; Lucania, G. Lidocaine-loaded non-ionic surfactant vesicles: characterization and in vitro permeation studies. *Int. J. Pharm.* **2002**, *231* (1), 21–32.